Materials Research Proceedings 69 (2026) 390-395 https://doi.org/10.21741/9781644904251-71

Trim Analysis of Highly Flexible Aircraft via a Coupled DG-VLM Framework

Elisa TESTAQUATRA[1,a], Vincenzo GULIZZI[1,b*]

[1]Department of Engineering, Università degli Studi di Palermo, Italy

[a]elisa.testaquatra@unipa.it, [b]vincenzo.gulizzi@unipa.it

Keywords: Flexible Aircraft, Hyperelasticity, Nonlinear Trim, Discontinuous Galerkin Method, Vortex Lattice Method

Abstract. An original computational framework for the trim analysis of highly-flexible aircraft is presented in this work. The framework is based on the combination of a discontinuous Galerkin (DG) method and a non-planar Vortex Lattice Method (VLM). The DG method is employed for solving three-dimensional finite-strain, whereas the non-planar VLM is employed for solving potential-flow aerodynamics of the deformed structure. The DG-VLM coupling is performed by considering the forces generated by the vortexes as energetically equivalent to body forces acting on the structure. The framework is validated by considering the finite-strain response of a cantilever beam, the finite-strain response of a highly flexible wing, and the angle of attack and elevator deflection at longitudinal trim condition of an aircraft featuring the same highly flexible wing.

Introduction

Over the past years, research on High Aspect Ratio Long Endurance (HALE) aircraft has been of particular interest, as high-aspect-ratio wings provide greater aerodynamic efficiency, reducing fuel consumption and extending endurance. However, high-aspect-ratio wings may undergo large deformations and rotations, which can significantly affect their aerodynamic characteristics. For this reason, the analysis and design of vehicles featuring such type of wings, including the aspects related to their flight mechanics performances, must be performed accounting for fluid-structure interaction effects.

Numerical methods are often necessary as analytical solutions are seldom available, especially in the regime of large deformations and rotations. Recently, several approaches have been proposed to solve the aeroelastic problems of highly flexible aircraft. Murua and Palacios [1] developed a computational framework based on a geometrically exact beam model and the Unsteady Vortex Lattice Method (UVLM). Zhang et al.[2] developed a 3D co-rotational beam framework, coupling the structural dynamics with unsteady aerodynamics. Drachinsky and Raveh [3] employed the modal rotation method to capture large deformations through spatial derivatives of mode shapes. Medeiros and Cesnik [4] proposed a reduced-order geometrically nonlinear formulation, accounting large deformation effects on both inertia and stiffness terms.

This contribution presents a novel computational framework for the aeroelastic analysis of highly flexible aircraft based on finite-strain elasticity and potential-flow aerodynamics. The framework is based on the coupling between a discontinuous Galerkin (DG) method for solving finite-strain total-Lagrangian elasticity and a non-planar Vortex Lattice Method (VLM) for solving potential flow aerodynamics. The framework is validated considering the finite-strain response of a cantilever beam and the finite-strain response of a highly flexible wing. Then, the framework is employed to study the longitudinal trim of an aircraft featuring a high-aspect-ratio wing. Numerical results are presented by comparing the computed values of angle of attack and elevator deflection at trim condition upon considering a rigid wing, an elastic wing undergoing small deformations, and an elastic wing undergoing large deformations.

Materials Research Proceedings 69 (2026) 390-395 https://doi.org/10.21741/9781644904251-71

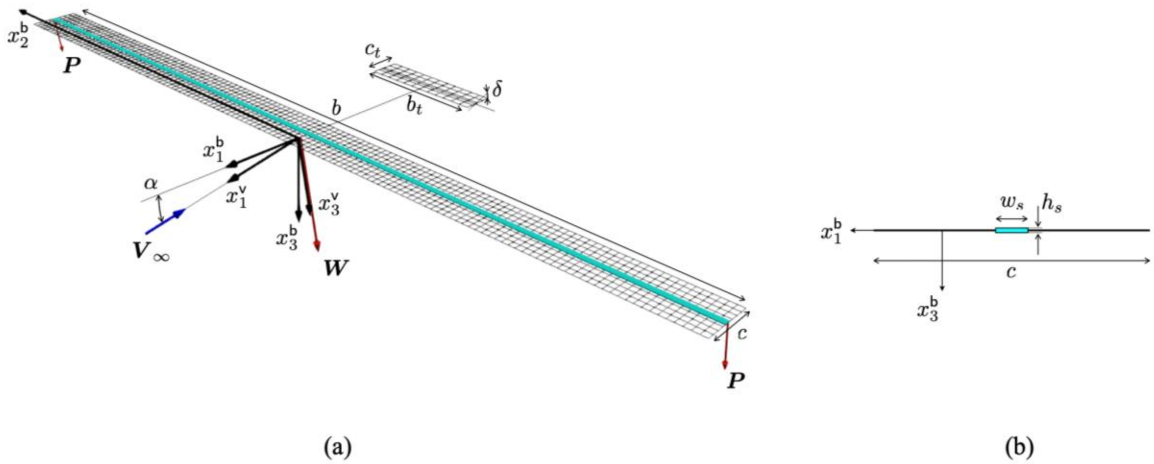

Figure 1: (a) Geometry of the flexible aircraft. (b) Load-bearing rectangular cross section of the main wing.

Problem statement

Let us consider the longitudinal behavior an aircraft modeled by a main wing and a horizontal tail, as shown in Fig.(1a). The span and the chord of the main wing are denoted by b and c, respectively, while the span and the chord of the horizontal tail are denoted by b_t and c_t, respectively. The main wing has a load-bearing rectangular cross section of density ρ_s, width w_s, and thickness h_s, that is placed at 50% of the wing's chord; see Fig.(1b). The entire horizontal tail is supposed to be a rigid movable surface that can rotate of an angle δ around an axis placed at 0.39% of its chord. The aircraft is assumed to be in horizontal flight at a speed V_∞ and angle of attack α within a fluid whose density is denoted by ρ_∞.

The flexible part of the aircraft is the load-bearing cross-section of the main wing, which is made of an isotropic material identified by Young's modulus E and Poisson's ratio ν. Two different elastic behaviors are considered for the main wing cross section, namely a linear elastic behavior within the small-deformation hypothesis and a hyper-elastic behavior accounting for large deformations and rotations. In the former case, the deformation of the main wing is obtained by solving the equations of linear elasticity combined with a constitutive behavior that can be written as $\boldsymbol{\sigma} = \boldsymbol{C}\boldsymbol{\varepsilon}$, where $\boldsymbol{\sigma}$ and $\boldsymbol{\varepsilon}$ are vectors collecting the stress and strain components, respectively, in Voigt notation, and $\boldsymbol{C}$ is the associated matrix of elastic coefficients for isotropic materials. On the other hand, in the hyper-elastic case, the deformation of the main wing is obtained by solving the equations of finite-strain elasticity in combination with a constitutive behavior of the form $\boldsymbol{S} = \boldsymbol{C}\boldsymbol{E}$, where $\boldsymbol{S}$ and $\boldsymbol{E}$ are vectors collecting the second Piola-Kirchhoff stress components and the Green-Lagrange strain components, respectively, in Voigt notation, whereas, following the Saint Venant–Kirchhoff model, $\boldsymbol{C}$ is the same matrix of elastic coefficients employed in the small-strain case.

The loads acting on the wing structure consist of its weight, a load $\boldsymbol{P}$ placed at each tip of the wing, and the aerodynamic loads deriving from the interaction with the fluid.

DG-VLM formulation

The solution of the aeroelastic problem introduced in the preceding section is performed by combining a DG formulation for solving finite-strain elasticity and a non-planar VLM for solving potential-flow aerodynamics. In this section, the solution of finite-strain is reported, whereas the solution of the rigid and small-strain problems can be obtained as special cases.

Following Gulizzi et al.[5], it is possible to show that the DG weak form associated to the finite-strain elastic behavior of the wing structure can be stated as follows: find $\boldsymbol{\varphi}$, being $\boldsymbol{\varphi}$ the approximated deformation mapping, such that $B(\boldsymbol{V},\boldsymbol{\varphi}) = F(\boldsymbol{V},\boldsymbol{b}_0)$ $\forall \boldsymbol{V} \in \boldsymbol{V}^{hp}$, being $\boldsymbol{V}^{hp}$ the space of discontinuous polynomial vector fields, where

$$B(\boldsymbol{V},\boldsymbol{\varphi}) \equiv \int_{\mathcal{D}^h} \frac{\partial \boldsymbol{V}^T}{\partial x_k}\frac{\partial w}{\partial \boldsymbol{F}_k} - \int_{\mathcal{J}^h}\left([\![\boldsymbol{V}]\!]_k^T \left\{\frac{\partial w}{\partial \boldsymbol{F}_k}\right\} + \{\boldsymbol{\Pi}_k^T\}[\![\boldsymbol{\varphi}]\!]_k \right) + \int_{\mathcal{J}^h} \mu [\![\boldsymbol{V}]\!]_k^T [\![\boldsymbol{\varphi}]\!]_k + \\ - \int_{\mathfrak{B}_D^h}\left(\boldsymbol{V}^T \frac{\partial w}{\partial \boldsymbol{F}_k} n_k + \boldsymbol{\Pi}_k^T n_k \boldsymbol{\varphi}\right) + \int_{\mathfrak{B}_D^h} \mu \boldsymbol{V}^T \boldsymbol{\varphi} \qquad (1)$$

and

$$F(\boldsymbol{V},\boldsymbol{b}) \equiv \int_{\mathcal{D}^h} \boldsymbol{V}^T \boldsymbol{b} \qquad (2)$$

In Eq.(1), w denotes the solid strain energy function, $\boldsymbol{F}_k$ denotes the k-th column of the deformation gradient tensor, n_k is the k-th component of the unit normal of the solid boundary, while $\boldsymbol{\Pi}_k$ is a symmetrization vector and μ is a penalization parameter that are typical of DG formulations. Additionally, the integrals appearing in Eq.(1) are referred to as broken integrals and must be intended as the sum over the mesh elements of the integrals computed over each element domain and boundary. See Ref.[5] for further details.

Eventually, Eq.(2) accounts for the loads acting on the wing structure and includes those stemming from gravity, the concentrated loads at the wing tips and the aerodynamic loads, which are computed solving a non-planar VLM system where the vortexes deform with the structure [6].

Upon introducing the DG structural degrees of freedom that are collected in the vector $\boldsymbol{X}$ and the VLM degrees of freedom that collected in the vector $\boldsymbol{\Gamma}$, the final system of equations governing the aeroelastic problem can be written as

$$\begin{cases} \boldsymbol{R}_S(\boldsymbol{X},\boldsymbol{\Gamma}) = \boldsymbol{0} \\ \boldsymbol{R}_A(\boldsymbol{X},\boldsymbol{\Gamma}) = \boldsymbol{0} \end{cases} \qquad (3)$$

where $\boldsymbol{R}_S(\boldsymbol{X},\boldsymbol{\Gamma})$ denotes the equations associated with the structural problem and $\boldsymbol{R}_A(\boldsymbol{X},\boldsymbol{\Gamma})$ denotes the equations associated with the aerodynamic problem. This system of equations is solved via a Newton-Raphson approach.

Results

In the first set of tests, an isolated half-wing with a load P placed at its tip is considered. The wing is clamped at its root and has a square cross section, i.e., $w_S = h_S$. Two lengths are considered, namely $b/2 = L = 10w_s$ and $b/2 = L = 100w_s$. The deformation of the structure using a kinematic model featuring a third-order approximation along the cross section and fifth-order approximation along the span. The obtained results are reported in Fig.(2) for the two lengths in terms of u_z/L versus $PL^2/(EI)$, where I is the moment of inertia of the cross section. The comparison with the results available in the literature [7,8] confirms the capability of the proposed framework to capture finite-strain bending behaviors.

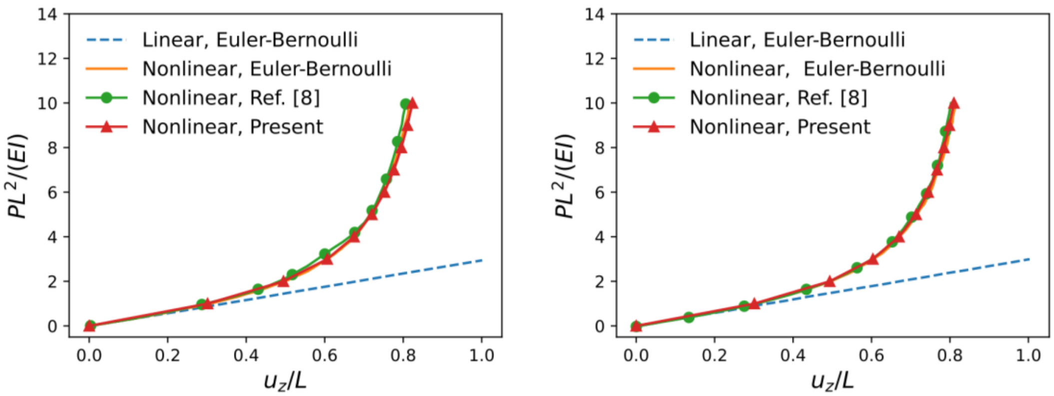

(a) (b)

Figure 2: Vertical displacement of a cantilever beam under finite deformations due to a tip load.

In second set of tests, the developed framework is employed to compute the aeroelastic response of a half-wing clamped at its root in terms of tip displacement versus wind speed. The wing is modeled under the small-strain hypothesis and under the finite-strain hypothesis. The geometrical and material properties of the considered wing can be found in Ref.[9]. The wing tip displacement as a function of the flow speed is reported in Fig.(3) for an angle of attack of 0.4°. The results obtained using the linear model and the nonlinear model are compared with the results (both numerical and experimental) provided in Ref.[9]. As shown in figure, it is possible to notice how the linear and nonlinear models agree for low speed, while they start to provide different results for a flow speed V_∞ approximately above 31 m/s, when the geometric nonlinearities become dominant. In particular, the linear models provide a tip displacement that tends to infinity as the flow speed approaches the divergence speed. Such a divergent behavior is not present in the results obtained by the nonlinear models, which remain much closer to the experimental results, confirming that the use of a finite-strain model is essential for accurately capturing the aeroelastic behavior of a highly flexible wing.

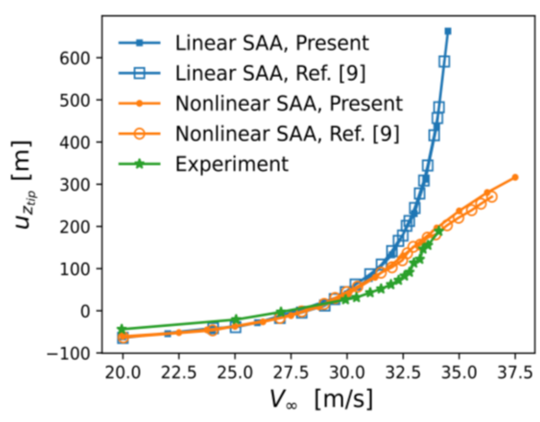

Figure 3: Wing tip displacement versus wind speed for a highly-flexible wing.

Eventually, the framework is employed to compute longitudinal trim conditions in terms of angle of attack and elevator deflection of an aircraft featuring the same highly flexible wing considered for the previous set of tests. The geometrical properties of the entire aircraft can be found in Ref.[10]. Table (1) reports the obtained values of angle of attack α and elevator deflection δ at longitudinal trim condition for $V_\infty = 25$ m/s in the cases the wing is considered rigid or highly flexible. An error of approximately 10% is observed with the results provided in the literature.

Materials Research Proceedings 69 (2026) 390-395 https://doi.org/10.21741/9781644904251-71

Table 1: Angle of attack α and elevator deflection δ at longitudinal trim condition for an aircraft featuring a highly-flexible wing for V_∞ = 25 m/s.

	Present		Ref.[10]	
	α [°]	δ [°]	α [°]	δ [°]
Rigid	3.77	-1.97	3.76	-1.98
Flexible	2.88	-1.99	3.22	-1.81

Conclusions

A novel computational framework for the trim analysis of highly-flexible aircraft has been presented. The novelty of the framework is the combined use of a discontinuous Galerkin method for solving finite-strain elasticity and a non-planar Vortex Lattice Method for solving potential-flow aerodynamics of the deformed structure. The capabilities of the framework have been assessed by analyzing the finite-strain bending of a cantilever beam subject to a tip load, the finite-strain aeroelastic response of an isolated wing, and the longitudinal trim of an aircraft featuring a highly-flexible wing. A satisfactory comparison between the results obtained with the present framework and the results available in the literature, which consist of both numerical and experimental results, has been observed. Currently the framework is being extended to consider different kinematic approximations, more complex internal structures and materials, and a wider range of flight conditions.

Acknowledgments

This work has been supported by the project “Hydro-dynamic devices for micro-particle trapping and vibrational energy harvesting (HYDRA)”, CUP B53D23005770006, funded by Next Generation EU - PNRR M4 - C2 - investimento 1.1: Fondo per il Programma Nazionale di Ricerca e Progetti di Rilevante Interesse Nazionale (PRIN) - PRIN 2022 cod.2022AALLEC.

References

[1] J. Murua, R. Palacios, J. M. R. Graham, Applications of the unsteady vortex-lattice method in aircraft aeroelasticity and flight dynamics, Progress in Aerospace Sciences. 55 (2012) 46-72. https://doi.org/10.1016/j.paerosci.2012.06.001

[2] C. Zhang, Z. Zhou, X. Zhu, L. Qiao, A comprehensive framework for coupled nonlinear aeroelasticity and flight dynamics of highly flexible aircrafts, Applied Sciences. 10(3)(2020) 949. https://doi.org/10.3390/app10030949

[3] A. Drachinsky, D. E. Raveh, Nonlinear aeroelastic analysis of highly flexible wings using the modal rotation method, AIAA Journal. 60(5) (2022) 3122-3134. https://doi.org/10.2514/1.J061065

[4] R. R. Medeiros, C. E. Cesnik, E.B. Coetzee, Computational aeroelasticity using modal-based structural nonlinear analysis, AIAA Journal. 58(1) (2020) 362-371. https://doi.org/10.2514/1.J058593

[5] V. Gulizzi, I. Benedetti, A. Milazzo, Discontinuous Galerkin methods for solids and structures, Comprehensive Structural Integrity 2nd edition, Oxford: Elsevier, (2023) 348-377. https://dx.doi.org/10.1016/B978-0-12-822944-6.00024-4

[6] V. Gulizzi, I. Benedetti, Computational aeroelastic analysis of wings based on the structural discontinuous Galerkin and aerodynamic vortex lattice methods, Aerospace Science and Technology, 144 (2024) 108808. https://doi.org/10.1016/j.ast.2023.108808

[7] K. E. Bisshopp, D. C. Drucker, Large deflection of cantilever beam, Quarterly of applied mathematics. 3(3) (1945) 272-275. https://www.jstor.org/stable/43633516

[8] A. Pagani, R. Augello, E. Carrera, Frequency and mode change in the large deflection and post-buckling of compact and thin-walled beams, Journal of Sound and Vibration. 432 (2018) 88-104. https://doi.org/10.1016/j.jsv.2018.06.024

[9] C. Xie, L. Wang, C. Yang, Y. Liu, Static aeroelastic analysis of very flexible wings based on non-planar vortex lattice method, Chinese Journal of Aeronautics. 26(3) (2013) 514- 521. https://doi.org/10.1016/j.cja.2013.04.048

[10] C. Yang, L. Wang, C. Xie, Y. Liu, Aeroelastic trim and flight loads analysis of flexible aircraft with large deformations, Science China Technological Sciences. 55(10) (2012) 2700-2711. https://doi.org/10.1007/s11431-012-4912-8